NUCL SCI TECH (2018) 29:171
https://doi.org/10.1007/s41365-018-0507-9

Development of large acceptance multi-purpose spectrometer in Korea for symmetry energy

Byungsik Hong[1] · Jung Keun Ahn[1] · Gyeonghwan Bak[2] · Jamin Jo[1] · Minho Kim[1] · Eun Joo Kim[3] · Young Jin Kim[4] · Young Jun Kim[1] · Minjung Kweon[5] · Hanseul Lee[2] · Hyo Sang Lee[4] · Jong-Won Lee[1] · Jung Woo Lee[1] · Kyong Sei Lee[1] · Byul Moon[1] · Dong Ho Moon[2] · Benard Mulilo[1] · Jaebeom Park[1] · Min Sang Ryu[4] · Hyunha Shim[1] · LAMPS Collaboration

Received: 6 August 2018 / Revised: 5 October 2018 / Accepted: 9 October 2018 / Published online: 10 November 2018

Abstract The Rare Isotope Accelerator complex for ON-line experiments (RAON) is a new radioactive ion beam accelerator facility under construction in Korea. The large acceptance multi-purpose spectrometer (LAMPS) is one of the experimental devices for nuclear physics at RAON. It focuses on the nuclear symmetry energy at supra-saturation densities. The LAMPS Collaboration has developed and constructed various detector elements, including a time projection chamber (TPC) and a forward neutron detector array. From the positron beam test, the drift velocity of the secondary electrons in the TPC is 5.3 ± 0.2 cm/μs with P10 gas mixture, and the position resolution for pads with dimensions of 4×15 mm^2 is in the range of $\sim$ 0.6–0.8 mm, depending on the beam position. From the neutron beam test, the energy resolution of the prototype neutron detector module is determined to be 3.4%, and the position resolution is estimated to be better than 5.28 cm. At present, the construction of the LAMPS neutron detector system is in progress.

Keywords RAON · LAMPS · Radioactive ion beam · Heavy-ion collision · TPC · Neutron detector · Nuclear symmetry energy · RCNP · ELPH

1 Introduction

With the advent of modern radioactive ion beam (RIB) accelerators, the investigation of various properties of nuclei and nuclear matter as a function of the isospin ratio has become possible. Exotic beams with very asymmetric neutron-to-proton ratio (*N*/*Z*) enable the study of the origin of the elements heavier than the most stable nuclei, such as Fe or Co, astrophysical processes along the edge of the nuclear chart, the unusual structure of nuclei near the drip lines, and the nuclear equation of state, particularly, the symmetry energy term [1–4].

The new RIB accelerators are characterized by high-intensity beams with an extreme *N*/*Z* ratio. Nearly a decade ago, Korea also joined the worldwide endeavor to construct a forefront RIB accelerator and various related experimental apparatus [5–7]. For this purpose, the rare isotope science project (RISP) was established at the Institute for Basic Science (IBS) in 2011. The ultimate aim of RISP is to construct a new RIB accelerator, known as the Rare Isotope Accelerator complex for ON-line experiments (RAON). In particular, RAON is expected to provide new opportunities to users not only for nuclear physics, but also for a wide range of applied research, including condensed

This work was supported by the National Research Foundation of Korea (NRF) Grants funded by the Korea government (MSIT) (2018M7A1A1053367, 2017M7A1A1019378, and 2013M7A1A1075765).

✉ Byungsik Hong
bhong@korea.ac.kr

[1] Department of Physics, Korea University, Seoul 02841, Republic of Korea

[2] Department of Physics, Chonnam National University, Gwangju 61186, Republic of Korea

[3] Division of Science Education, Chonbuk National University, Jeonju 54896, Republic of Korea

[4] Rare Isotope Science Project, Institute for Basic Science, Daejeon 34047, Republic of Korea

[5] Department of Physics, Inha University, Incheon 22212, Republic of Korea

matter physics, biology, medical applications, and the production of new nuclear reaction data.

In this paper, first we briefly introduce RAON in Sect. 2 and the large acceptance multi-purpose spectrometer (LAMPS) in Sect. 3, which is one of the experimental devices for nuclear physics. Then, the development of the two detector elements used in the LAMPS, the time projection chamber (TPC) and the neutron detector array (NDA), is discussed in Sects. 4 and 5, respectively. Finally, Sect. 6 summarizes the paper.

2 Overview of RAON

The RAON facility utilizes two different RIB production methods: the in-flight fragmentation (IF) and the isotope separator on-line (ISOL). The ISOL system is driven by a cyclotron providing 70 MeV proton beams with a current of 1 mA. When the low-density porous UC_x target is bombarded by protons, radioactive isotopes are generated in the direct fission of ^{238}U. Then, a post-accelerator increases the beam energy up to $\sim$ 18.5 MeV/u for the low-energy experiments.

The IF system of RAON is driven by heavy U beams. The U^{+79} beams are accelerated up to 200 MeV/u at the end of the superconducting driver linear accelerator (LINAC) and collide with the production target for projectile fragmentation. The desired radioactive ions are selected by the pre- and main separators and collide with the experimental target in the detector system, such as the LAMPS. For particle identification, a parallel plate avalanche chamber (PPAC), a plastic scintillation detector, and a slit system are installed at each focal point.

The ISOL and IF systems can be operated independently; nevertheless, a unique feature of RAON is the combination of the two methods. Specifically, the radioactive ion beams from ISOL are introduced to the driver LINAC and bombard the IF target, which produces more exotic RIBs that cannot be obtained by either ISOL or IF exclusively. According to the simulation, the intensities of certain exotic nuclei are several orders of magnitude higher in combined operation than those obtained by using IF exclusively [8]. As a result, a combination of the ISOL and IF systems widens the range of application of the nuclear physics research in the future.

RAON provides several experimental areas for users in different fields [7, 9]. A overview of the representative experimental apparatuses for each area is given in Table 1 together with the relevant research topics. The scientific aim of RAON is quite broad, ranging from the fundamental structure of exotic nuclei to various applications, such as medical science and condensed matter physics. The locations for experimental nuclear physics are the low-energy hall and the high-energy hall A, where the KOrea Broad acceptance Recoil spectrometer and Apparatus (KOBRA) and LAMPS systems are planned to be installed, respectively. In the following sections, the progress of the development of certain hardware components of the LAMPS system is presented.

3 Overview of LAMPS

The main aim of LAMPS is to investigate the density dependence of the nuclear symmetry energy, which is the difference between the energy of the pure neutron matter and that of the isospin symmetric ($N = Z$) matter [10]. When the nuclear symmetry energy is expanded in series in terms of the baryon density around the saturated value (ρ_0), the coefficients of the first (slope of L) and the second (curvature of K_{sym}) terms denote pressure and compressibility, respectively, from the symmetry energy. Certain experimental data are currently available to constrain L and K_{sym} near ρ_0; however, detailed information, especially for dense matter are still highly desired. Therefore, the LAMPS is expected to provide precision data to narrow down the range of L and K_{sym} for the ρ_0 densities mentioned above.

The nuclear symmetry energy is essential to understand the many-body theory of a strongly interacting nuclear

Table 1 Summary of experimental configurations and their scientific aims at RAON

Experimental areas	Experimental apparatus	Scientific aims
Ultra-low-energy hall	High-precision mass-measurement system (HPMMS)	Properties of exotic nuclei
	Collinear laser spectroscopy system (CLS)	Fundamental symmetries
Low-energy hall	KOBRA recoil spectrometer	Properties of exotic nuclei
	Neutron science facility	Nuclear data measurement
High-energy hall A	LAMPS	Nuclear symmetry energy & structure
High-energy hall B	μSR system	Condensed matter physics
	Biology and medical science facility	Biology and medical research

system, which is closely related to the various astrophysical objects, such as neutron stars and supernovae [2, 10]. Experimentally, radioactive ion beams are indispensable for the detailed investigation of the nuclear symmetry energy, because they can generate nuclear matter with extraordinary *N*/*Z* ratios. Therefore, the LAMPS system in RAON will play an important role in the future study of the symmetry energy [6, 7].

Figure 1 shows a schematic of the complete LAMPS device, which is a combination of a solenoid system, a dipole system, and a forward neutron detector array (it should be noted that the construction of the dipole spectrometer and the Si–CsI detector component in the solenoid spectrometer has been postponed to the second stage due to a budget constraint). The most important characteristic of the LAMPS device is to detect various probes simultaneously. Protons and $\pi^{\pm}$ can be measured by a large acceptance ($> 3\pi$) TPC in a superconducting magnet [11]. The light fragments can possibly be measured by the TPC with a reduced gain. Neutrons are measured by the neutron detector array in the very forward region (the beam fragments with large *Z* values are also planned to be detected; however, these measurements cannot be performed until the dipole spectrometer is available). Therefore, the LAMPS device enables a comprehensive analysis of various observables for the nuclear symmetry energy, such as the yield ratio of neutrons and protons, π^{-}/π^{+} ratio, isospin diffusion parameter, and collective flow. In the following, the current status of certain hardware components of the LAMPS system is discussed. In particular, the status of the TPC and the neutron detector array with the novel dedicated electronics is detailed.

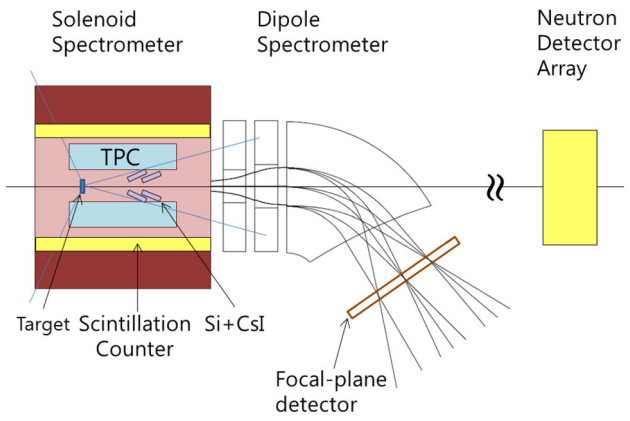

Fig. 1 (Color online) Schematic of the LAMPS at RAON [6, 7]. The construction of the dipole spectrometer and the Si–CsI array are currently postponed to the second phase

4 Time projection chamber

The TPC is a three-dimensional tracking detector utilizing the drift time of the ionized electrons in a gas mixture [12]. Figure 2 shows a schematic of the structure and dimensions of the LAMPS TPC. It covers the laboratory polar angle (θ_{lab}) in the range of 24°–127° because the nominal target position is located 30 cm from the upstream edge of the TPC. The gas mixture is contained by a cylindrical vessel with a length of 1.2 m and the radius of 50 cm. The gas vessel has a cylindrical hole with a radius of 15 cm along the beam axis to avoid the saturation with beam particles. An optional membrane for high-voltage application can be inserted in the middle of the gas vessel if the signals are read out at both endcaps. In the current configuration, the electric and magnetic fields in the TPC are parallel.

In the LAMPS TPC, a gas-electron multiplier (GEM) is used for signal amplification [13]. Each end of TPC is equipped with three GEM foils. The employed GEM foil was originally developed by the Korean vendor for the Compact Muon Solenoid (CMS) Collaboration at the Large Hadron Collider (LHC), at CERN [14]. In each GEM foil a 50 μm thick Kapton foil is sandwiched by two 5 μm thick copper planes. The radius of each GEM hole is $\sim$ 35 μm, and their pitch is 57.5 μm. The GEM foil is manufactured in a factory as a roll with a total length of $\sim$ 1–2 km. The uncertainty of the thickness of the GEM foil, which is one of the important factors determining the uniformity of the amplification, is less than 1 μm for one role. Another important factor to determine the uniformity of the amplification is to maintain a uniform distance between the neighboring two foils in the triple GEM system. The CMS Collaboration requires an overall uncertainty (standard deviation) of the amplification factor of less than 16%, and we use the GEM foils that satisfy the CMS criterion.

Prior to the construction of the real-size TPC, the LAMPS group built a prototype to understand the details of

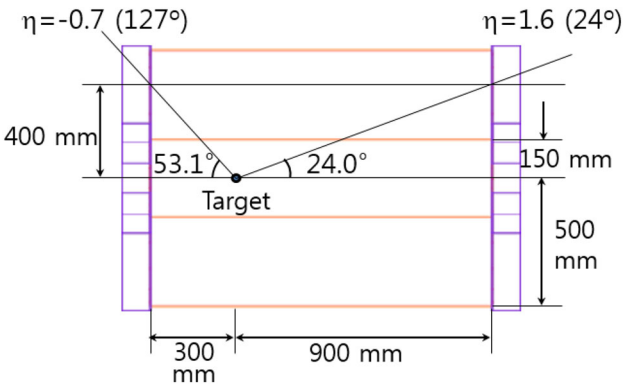

Fig. 2 (Color online) Schematic drawing of the LAMPS TPC, obtained from Ref. [6]

its performance. All dimensions of the prototype LAMPS TPC were approximately one half of those of the real-size TPC, with a length and outer radius of 57.0 and 24.5 cm, respectively. A readout pad plane is installed on one end, and a high-voltage (HV) cathode plane is installed on the other end of the gas vessel. The overall shape of the readout plane is octagonal, consisting of eight isosceles trapezoidal sectors arranged azimuthally. The shape of each pad is rectangular. The dimensions of the pads were 3×10 mm^2 for the small radius region and 4×15 mm^2 for the large radius region. Out of the eight sectors, only four of them were filled.

We installed the prototype LAMPS TPC at the research center of ELectron and PHoton science (ELPH) at Tohoku University, Japan, in November 2016. Positron beams of 500 MeV were utilized to study various properties of the prototype TPC, such as the drift velocity and position resolution, as shown in Fig. 3. The TPC could be moved vertically by a jackscrew to change the beam entrance position. The beam trigger was defined by six scintillator counters. Two counters with widths of 1 cm for each defined 1×1 cm^2 beam size located right upstream of the TPC, and a relatively wide scintillator with a width of 4 cm, located at the downstream of the detector, generated the beam trigger signals. In addition to the two large paddles with dimensions of 20×20 cm^2 were placed upstream and downstream of the TPC for redundancy. For the experiment, two different gas mixtures were tested: 90% Ar mixed with either 10% CH_4 (P10) or 10% CO_2 (C10). However, only the data for P10 are presented in this paper.

Fig. 3 (Color online) Picture of the experimental setup at the ELPH. The prototype TPC is installed vertically in the center. The TPC can move vertically to change the beam injection position in it. The trigger counters are installed at the entrance and exit of the beam in TPC, and the readout electronics can be seen in the adjacent racks

Figure 4 shows a few examples of the event display for positron beams at 500 MeV. Due to the absence of the applied magnetic field, all tracks are straight lines (the color code on the right side represents the amount of energy loss detected by each pad). As described before, the prototype TPC moved vertically to vary the entrance position of the beam particles along the symmetry axis, which changes the drift length of the secondary electrons to the pad plane.

4.1 Drift velocity

Figure 5 shows the measured correlation between the height of the beam position, h, and the arrival time, t_{arrival}, for P10 at an electric field strength of 155 V/cm. The two variables exhibit a perfectly linear relationship as indicated by the solid line. The fitted slope parameter represents the drift velocity, v_{drift}, which is 5.3 ± 0.2 cm/μs. With this value of v_{drift}, the maximum distance for the secondary electrons to be recorded is ~ 1 m in the current setup of the General Electronics for TPCs (GET) [15]: 512 bins (maximum number of the digitized data sets of the buffer memory for one channel) $\times 0.04$ μs/bin (inverse of 25 MHz sampling rate) $\times 5.3$ cm/μs (v_{drift}) $\simeq 1$ m. Therefore, for the real-size LAMPS TPC, which is 1.2 m long, the secondary electrons generated in one end of TPC cannot reach the pad plane on the other end within one period of buffer memory. In this case, the HV membrane in the middle of TPC is necessary to record signals at both ends.

Figure 6 shows a compilation of the data for the drift velocity as a function of the electric field strength for P10, along with the simulation results obtained using the Garfield++ simulation toolkit with the LAMPS TPC geometry [11, 16]. In general, the experimental data for P10 are reproduced reasonably well by the simulation. The drift velocity distribution for P20 was also simulated, as shown by the open squares in Fig. 6: the drift velocity was

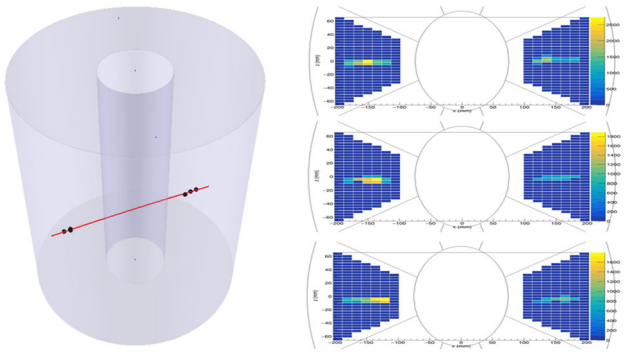

Fig. 4 (Color online) Examples of the TPC event display for positron beams at 500 MeV provided by the ELPH. Due to the absence of a magnetic field, all tracks are straight lines. The color code on the right displays the amount of energy loss detected by each pad

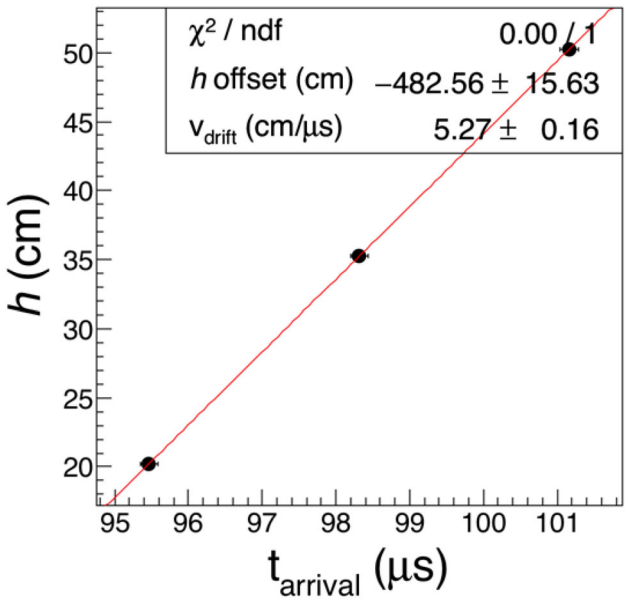

Fig. 5 (Color online) Correlation between the beam height position (h) and arrival time (t_{arrival}) for P10 (preliminary). For this particular example, the electric field strength in the TPC was 155 V/cm. The solid line represents a linear fit to the data points, and the slope parameter corresponds to the drift velocity v_{drift} of the ionized secondary electrons

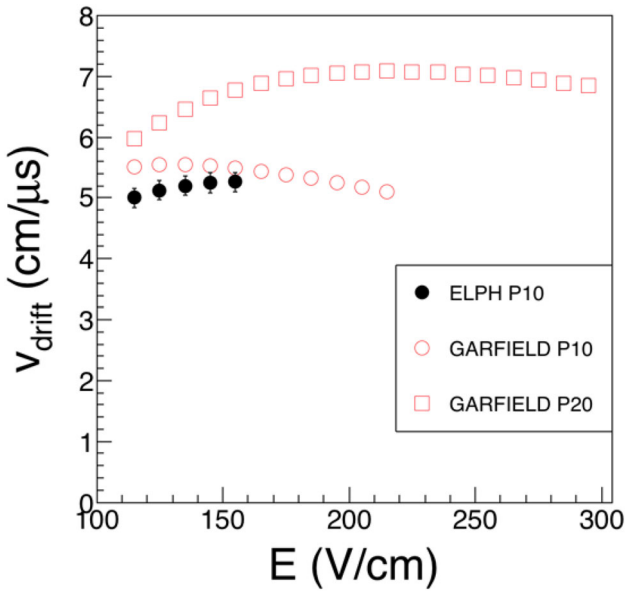

Fig. 6 (Color online) Drift velocity distribution of the secondary electrons in the prototype TPC as a function of the electric field strength for P10 (preliminary). The open symbols are the simulated data using the Garfield++ simulation toolkit

~ 6 cm/μs at 115 V/cm and increased to ~ 7 cm/μs at 175 V/cm. If $v_{\text{drift}} > 6$ cm/μs, the maximum distance for the secondary electrons to be recorded in each event is larger than 1.2 m, which is the length of the gas vessel for the LAMPS TPC. As a result, a readout pad is sufficient only at one end without the HV membrane.

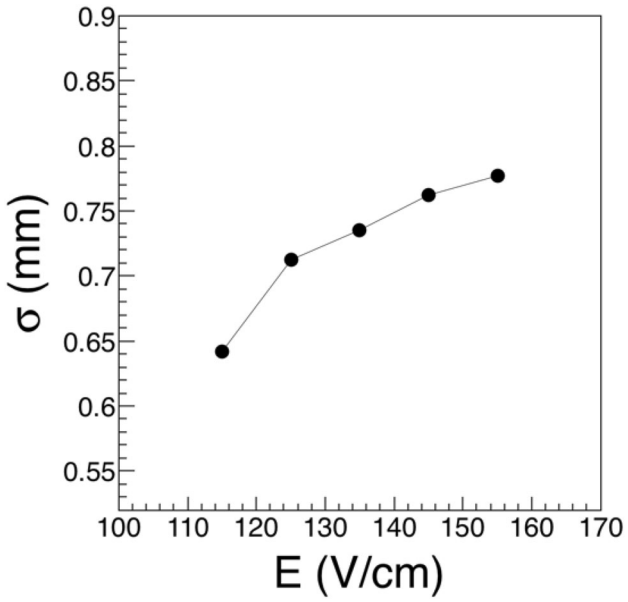

Fig. 7 Position resolution, σ, in the middle of the prototype TPC ($h = 35$ cm) as a function of the strength of electric field for P10 (preliminary). The fitting errors are smaller than the symbol size

4.2 Position resolution

The position resolution is obtained from the residual distribution where the residue is defined by the difference between the position of hit and the projected position of each reconstructed track. The residual distributions are described appropriately by Gaussian functions near the peak. The width parameter σ of the Gaussian fit function to the residual distribution is defined as the position resolution.

Figure 7 shows the position resolution, σ, of the prototype TPC for P10 as a function of the electric field strength. The data in Fig. 7 were obtained for larger pads (4×15 mm^2) when the e^+ beams enter the central position of the TPC ($h = 35$ cm). The position resolution is distributed in the range of 0.6–0.8 mm, depending on the electric field strength. It was observed that the smaller field strength provided a better position resolution. It should be noted that the position resolution for a smaller pad size (3×10 mm^2) is significantly better than that for larger pads by at least a factor of three.

The position resolution along the drift direction, which is estimated to be $\sim$ 3%, is determined by the uncertainties of the arrival time and the drift velocity. Thus, the position resolution of hits in the central region is $\sim$ 9 mm. However, it should be noted that the beam passes through the LAMPS TPC along the symmetry axis; thus, the

position resolution on the pad plane (Fig. 7) is the most important parameter for the uncertainty in the track (and subsequently momentum) reconstruction in the real experiment.

5 Neutron detector array

The forward NDA for the LAMPS consists of four stations with a veto wall. Each station consists of two layers, and each layer consists of twenty scintillator bars (The dimension of each scintillator bar is $10 \times 10 \times 200$ cm^3). The scintillator bars are made of polyvinyltoluene-based BC-408, obtained from Saint-Gobain Crystals, Inc., which is characterized by a relatively fast timing response and narrow pulse width [17]. In each station the scintillator bars are arranged in vertical and horizontal directions for the upstream and downstream layers, respectively, to provide two-dimensional hit information. A veto wall is positioned at the right upstream of the neutron detector array to remove charged particles. The dimensions of the veto wall are the same as those of an NDA layer except for the thickness, which is 5 cm. The overall structure of the NDA is shown in Fig. 8. The signals from each bar are read out by a photomultiplier tube (PMT) at both ends. In each module, an acrylic light guide is installed between the scintillator bar and the PMT for the collection of scintillation lights.

Previously, the prototype detectors were constructed and their performance was tested using radiation sources [18, 19]. However, because the mean kinetic energy of neutrons from ^{252}Cf is only $\sim$ 1.7 MeV, the further investigation of the performance at significantly higher kinetic energies at a few hundreds MeV is strongly desired. Therefore, we set up a small neutron detector array using several prototype detectors at the N0 beamline, dedicated to neutron beam research, at the Research Center for Nuclear Physics (RCNP) in Japan, as shown in Fig. 9.

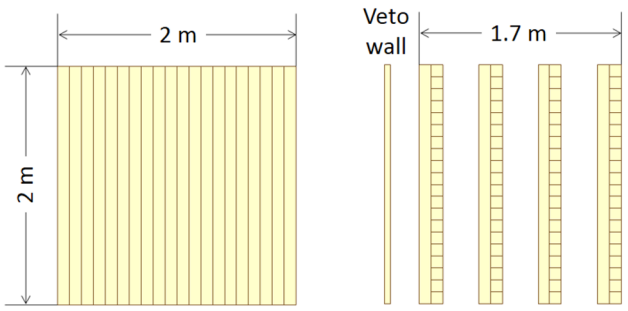

Fig. 8 (Color online) Overall structure of the forward neutron detector array for LAMPS. The left figure is a view from the beam direction and the right figure is a view from the side, obtained from Ref. [6]

For the current test, the prototype detectors were arranged in three stations with a veto counter in the front. The first station consists of two scintillator bars with dimensions of $10 \times 10 \times 100$ cm^3 and with each positioned vertically. The second station consists of the four real-sized scintillator bars with dimensions of $10 \times 10 \times 200$ cm^3 and with each positioned horizontally. Finally, the last station consists of the four block-type scintillators with

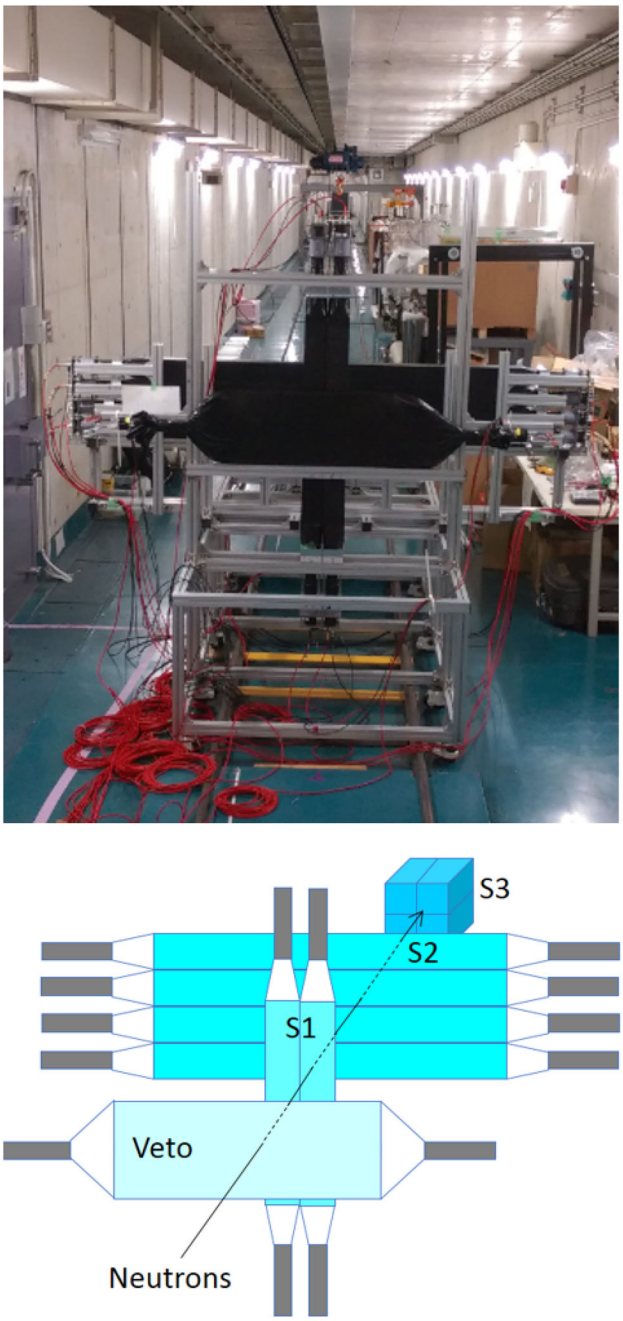

Fig. 9 (Color online) (Top) Picture of the experimental setup for the miniature NDA system at RCNP. (Bottom) Schematic drawing of the detector setup for the neutron beam test at RCNP

dimensions of $10 \times 10 \times 20$ cm^3 each. The gap between the stations was 60 cm. The veto detector was a scintillator plate with a thickness of 5 mm, and its area was sufficiently large to cover the whole beam area on the detectors. A schematic diagram of the detector setup at RCNP is shown in the bottom of Fig. 9.

For the readout electronics of the NDA, a dedicated flash analog-to-digital converter (FADC) was developed by a local vendor. This FADC supplies the timing and pulse-shape information at the same time, which enables us to perform a more sophisticated pulse-shape analysis when necessary. The dynamic range of analog input is from approximately $-$ 2 V to 0 V aby default, but the range can be extended to 2 V for both the positive and negative polarities by adjusting the ground level. The FADC has a sampling rate of 500 MHz with a resolution of 12 bit for the charges and a 125 MHz sampling rate with a 10-bit resolution for the timing information. The times were recorded for a duration of 16 s for each 8 ps interval. Including other uncertainties, the overall timing resolution of the electronics alone was measured to be in the range of $\sim$ 20–40 ps. Because we expect the timing resolution of each NDA module to be a few 100 ps, a timing resolution with 10 bit is sufficiently fine enough the LAMPS neutron detector. For the discrimination of multiple neutrons, the consecutive pulses are needed to be separated by at least 32 ns for a single neutron incident event.

5.1 Energy resolution

Within each event, most of the neutrons give the energy loss information (dE/dx) to only one detector module. However, neutrons occasionally give the energy loss information simultaneously to two modules when they entering the boundary of two adjacent detectors. For the position resolution analysis, we used only these special events.

Figure 10 shows the kinetic energy spectrum. The kinetic energy of neutrons was calculated by the relativistic formula $E_{\mathrm{n}} = (\gamma - 1)m_{\mathrm{n}}c^2$, where $\gamma = [1 - (l/t^{\mathrm{n}}_{\mathrm{ToF}}c)^2]^{-1/2}$ is the Lorentz factor with path length l and flight time $t^{\mathrm{n}}_{\mathrm{ToF}}$, while $m_{\mathrm{n}}c^2$ is the rest mass of neutron. In the above formula for E_{n} all uncertainties are contained by the measured variable $t^{\mathrm{n}}_{\mathrm{ToF}}$.

The distribution, which is nearly flat on the lower energy side of the major peak, is obtained from the beam energy dispersion and the room scattered components or products from various nuclear interaction channels. As we are only interested in the neutrons with incident energies, the peak near the bombarding energy in Fig. 10 is fitted by the Gaussian function. The value of $\sigma(E_{\mathrm{n}})$ for the fitted Gaussian function is 5.62 MeV; thus, the energy resolution

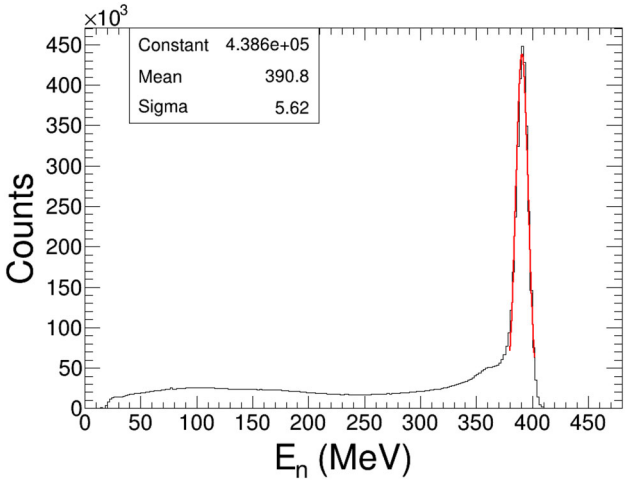

Fig. 10 (Color online) Measured kinetic energy spectrum of neutrons at 392 MeV (preliminary). The solid red line is a Gaussian function fitted to the peak at incident energy

is estimated to be $R_{\mathrm{E}}(n) = FWHM(E_{\mathrm{n}})/E_0 = 3.4\%$. Currently, more thorough analysis, for example, the deconvolution of the energy dispersion of the neutron beam, is being performed.

5.2 Position resolution

The distribution of the position differences (Δx) between the two vertically positioned scintillators in the first station at 392 MeV is shown in Fig. 11. A threshold of 10 MeV is required for all hits and the two hits are required to be within 3 ns, which ensures that they are from the same event. As shown by the solid red line in Fig. 11 the peak is described appropriately by the Gaussian function. The value of σ for the fitted Gaussian function is 4.49 cm; therefore, dividing by $\sqrt{2}$ the σ value of each scintillator bar is estimated to be 3.17 cm, assuming that the two detectors possess exactly the same properties. However, this result needs to be considered as a worst-case limit because the recoiled protons from one detector are assumed to be transferred to the next one horizontally. In reality, as the recoiled protons enter the next scintillator under certain angles, the intrinsic position resolution is expected to be better than 3.17 cm. In the future, a more accurate estimation of the position resolution using narrow trigger counters or cosmic rays is necessary.

5.3 Construction of the NDA system

The LAMPS Collaboration started the assembly of all NDA modules in early 2018 and plans to finish the work by the end of the same year. Figure 12 shows pictures of the assembly procedure. The assembly procedure can be summarized as follows:

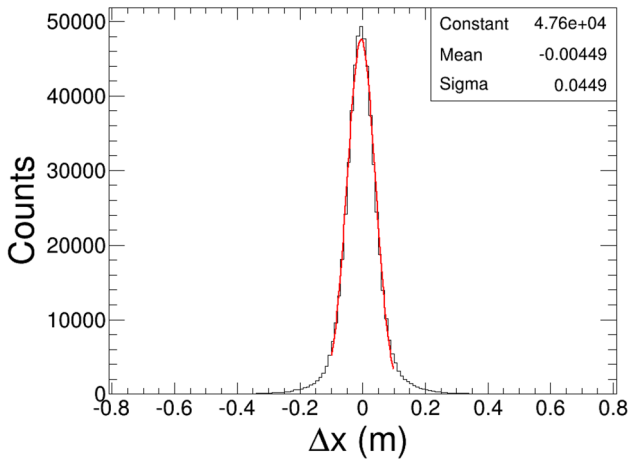

Fig. 11 (Color online) Hit position difference between the two vertical scintillators in the first station at 392 MeV (preliminary). The solid red line is the Gaussian function fitted to the peak

- The scintillator bar is first wrapped by a reflecting film and then by a black sheet to prevent the transmission of light from the scintillating material to the environment or vice versa. The leakage of scintillating light results in a severe deterioration of signal pulses, and the background light infiltrated from outside generates unwanted noise.
- Owing to its fast hardening of only a few minutes, an ultraviolet (UV) sensitive glue is used to temporarily attach the scintillator bar and the light guide. This procedure is necessary to attach them during the long curing process by the high-quality glue.
- Before applying the UV sensitive glue to the periphery of the interface, the high-quality glue, which requires at least 24 h to be hardened, needs to be applied to the interface. The amount of the 24-h glue is very important to avoid excessive leakage when the two parts are pressed by the vice.
- When the wrapping and gluing processes are completed, the assembled modules are installed in the frame. The frame is prepared for each station, and the veto wall is installed in the first frame. The frame is also equipped with pieces that hold and press the PMT on the light guide.
- After each frame is completed, the test with cosmic ray muons is performed to characterize certain basic properties, such as the detection efficiency and time and position resolutions. All information, such as characteristics of the NDA modules, conditions for the PMT operation, and noise levels for each detector, are recorded in the database.

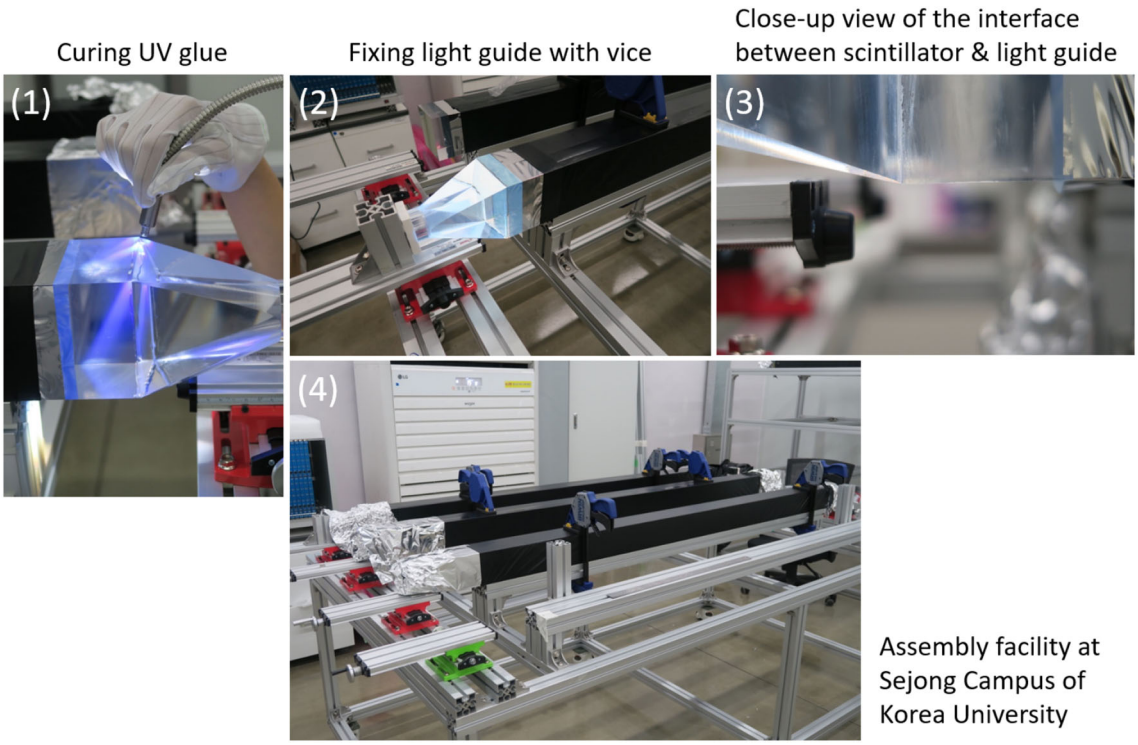

Fig. 12 (Color online) Assembly procedure of NDA modules: (1) Curing UV glue for temporary hardening of the scintillator bar and light guide and (2) pressing the light guide on the scintillator bar for permanent hardening with high-quality 24-h glue. (3) Close-up picture of the interface between the scintillator bar and light guide. (4) Storage facility of the assembled detector modules

6 Summary

The advanced radioactive ion beam accelerators including RAON in Korea open a new chapter in nuclear physics, by enabling the study of, for example, the origin of heavy elements, astrophysical processes, the interesting structure of nuclei near drip lines, and the nuclear symmetry energy. RAON is the first internationally recognized accelerator system for nuclear physics in Korea. The two major experimental systems for nuclear physics are KOBRA and LAMPS: KOBRA is a recoil spectrometer for nuclear structure and astrophysics at low energies (a few MeV/u) and LAMPS is a large acceptance spectrometer focusing on nuclear symmetry energy and structure at $\sim$ 250 MeV/u.

Using the LAMPS system enables the study of the density dependence of the nuclear symmetry energy in details, especially, at supra-saturation densities. Considering this aim, the LAMPS Collaboration has actively developed and constructed various detector components. Among these, the development and status of the TPC and the NDA have is presented in this paper.

We built a one half scale prototype TPC, which employs triple GEM foils, originally developed for the CMS Collaboration at CERN. The prototype TPC was shipped to ELPH in Japan to test certain basic properties, such as the drift velocity and position resolution, using e^+ beams at 500 MeV. By analyzing the data for different beam positions, the drift velocity of the secondary electrons in the TPC was determined to be 5.3 ± 0.2 cm/μs with the P10 gas mixture. The position resolution of the prototype TPC for the pads with dimensions of 4×15 mm^2 were in the range of 0.6–0.8 mm, depending on the strength of electric field. For smaller pads (3×10 mm^2) the position resolution was improved by at least a factor of three.

We also built the prototype detector modules for NDA and shipped them to RCNP in Japan for testing the various properties using neutrons beams at 392 and 65 MeV (This paper discussed only the 392-MeV results). The energy resolution (the full width at half maximum of the peak in the reconstructed energy distribution) is determined as 3.4%, and the position resolution is estimated to be better than 5.28 cm. At present, the construction of the LAMPS NDA is in progress in the laboratory at the Sejong Campus of Korea University.

References

1. B.A. Li, Probing the high density behavior of the nuclear symmetry energy with high energy heavy-ion collisions. Phys. Rev. Lett. **88**, 192701 (2002). https://doi.org/10.1103/PhysRevLett.88.192701
2. A.W. Steiner, M. Prakash, J.M. Lattimer et al., Isospin asymmetry in nuclei and neutron stars. Phys. Rep. **411**, 325–378 (2005). https://doi.org/10.1016/j.physrep.2005.02.004
3. W. Reisdorf, D. Best, A. Gobbi et al., Central collisions of Au on Au at 150, 250 and 400 A·MeV. Nucl. Phys. A **612**, 493–556 (1997). https://doi.org/10.1016/S0375-9474(96)00388-0
4. B. Hong, N. Herrmann, J. Ritman et al., Stopping and radial flow in central ^{58}Ni+^{58}Ni collisions between 1A and 2A GeV. Phys. Rev. C **57**, 244–253 (1998). https://doi.org/10.1103/PhysRevC.57.244
5. Rare Isotope Science Project. http://www.risp.re.kr/eng/orginfo/intro_project.do. Accessed 8 Nov 2018
6. B. Hong, J.K. Ahn, Y. Go et al., Plan for nuclear symmetry energy experiments using the LAMPS system at the RIB facility RAON in Korea. Eur. Phys. J. A **50**, 49 (2014). https://doi.org/10.1140/epja/i2014-14049-2
7. B. Hong, Prospects of nuclear physics research using rare isotope beams at RAON in Korea. Nucl. Sci. Technol. **26**, S20505 (2015). https://doi.org/10.13538/j.1001-8042/nst.26.S20505
8. J.W. Shin, K.J. Min, C. Ham et al., Yield estimation of neutron-rich rare isotopes induced by 200 MeV/u ^{132}Sn beams by using GEANT4. Nucl. Instrum. Methods B **349**, 221–229 (2015). https://doi.org/10.1016/j.nimb.2015.03.005
9. K. Tshoo, Y.K. Kim, Y.K. Kwon et al., Experimental systems overview of the Rare Isotope Science Project in Korea. Nucl. Instrum. Methods B **317**, 242–247 (2013). https://doi.org/10.1016/j.nimb.2013.05.058
10. B.A. Li, L.W. Chen, C.M. Ko, Recent progress and new challenges in isospin physics with heavy-ion reactions. Phys. Rep. **464**, 113–281 (2008). https://doi.org/10.1016/j.physrep.2008.04.005
11. G. Jhang, J.W. Lee, B. Moon et al., Simulation of the time-projection chamber with triple GEMs for the LAMPS at RAON. J. Korean Phys. Soc. **68**, 645–652 (2016). https://doi.org/10.3938/jkps.68.645
12. J.N. Max, D.R. Nygren, The time projection chamber. Phys. Today **3**(1), 46–53 (1978). https://doi.org/10.1063/1.2994775
13. F. Sauli, GEM: a new concept for electron amplification in gas detectors. Nucl. Instrum. Methods A **386**, 531–534 (1997). https://doi.org/10.1016/S0168-9002(96)01172-2
14. CMS Collaboration. The Phase-2 Upgrade of the CMS Muon Detectors. CMS-TDR-016 (2017)
15. J. Giovinazzo, T. Goigoux, S. Anvar et al., GET electronics samples data analysis. Nucl. Instrum. Methods A **840**, 15–27 (2016). https://doi.org/10.1016/j.nima.2016.09.018
16. Garfield++: simulation of tracking detectors. http://garfieldpp.web.cern.ch/garfieldpp. Accessed 8 Nov 2018
17. Saint-Gobain Crystals. https://www.crystals.saint-gobain.com/. Accessed 8 Nov 2018
18. K. Lee, K.S. Lee, B. Hong et al., Performance of a real-size prototype neutron detector for the LAMPS at RAON. J. Korean Phys. Soc. **65**, 610–615 (2014). https://doi.org/10.3938/jkps.65.610
19. K. Lee, K.S. Lee, B. Mulilo et al., Source test of the prototype neutron detector for the large-acceptance multipurpose spectrometer at RAON. J. Korean Phys. Soc. **62**, 1227–1232 (2013). https://doi.org/10.3938/jkps.62.1227